52nd IEEE Conference on Decision and Control
December 10-13, 2013. Florence, Italy

Achievable Performances for Basic Perturbation-Based Extremum Seeking Control in Wiener-Hammerstein Plants

Jean-Sébastien Deschênes, and Pierre N. St-Onge

Abstract— **This paper presents a case study for determining achievable performances in the basic form of extremum seeking control. Despite recent developments on more powerful versions of the algorithm, no detailed study that investigates this aspect thoroughly and provides clear guidelines for the tuning of this simpler, readily-implementable version is yet available. Interest remains for this basic version, for a variety of reasons. A review of extremum seeking fundamentals, with the support of a few simulations, allows to determine better means of selecting the elementary loop components, maximizing the gradient capture information. The choice of the excitation (dither) fundamental frequency is also better addressed under this optimal condition to effectively discuss achievable loop performance aspects. Most results apply to Wiener-Hammerstein classes of systems (strictly proper and stable system dynamics) and still allow other loop improvement modifications to be applied. Extensions to square wave dither signals and a few comparisons with other recently developed loop improvement techniques are also provided.**

I. Introduction

Extremum seeking control (ESC), even in its most simple form (perturbation-based approach from [1]), still receives a lot of attention in the literature [2, 3, 4]. Its main advantage of not being model-based and requiring minimal information about the system to optimize has fostered numerous practical applications of the technique (e.g. [5, 6, 7]). Despite recent progress in the field, there still lacks convenient methods for tuning the ESC and improving its transient performances [8, 9, 10]. As it is often emphasized, small improvements on this level can have significant economic impacts [11, 12]. These facts have motivated the development of various methods for circumventing the inherent limitations of perturbation-based ESC, for example, performing the gradient estimation with a recursive least squares (RLS) algorithm [13], adaptive filters [4, 14], windowing functions [15], etc. However, achievable performances of the basic version of the ESC still remain to be determined to establish better comparisons.

Many implementations of ESC imply a triple time-scale separation between system dynamics, dither fluctuations and plant input variations. Though this has to be the case in some situations (non-Wiener-Hammerstein systems), this results in very poor performances that may be impractical for real-life applications. Wiener-Hammerstein situations do not require such time-scale separation [9, 16], and the dither oscillations can very well be in the system's natural dominant frequency range. In [14], a fast extremum-seeking scheme is developed for application to Wiener-Hammerstein situations, where the dither frequency can even be far above the system dominant poles. This very recent development confirms the feasibility of applying higher frequency dithers to Wiener-Hammerstein systems, and the sustained interest for further developments applicable to this class of systems.

This paper is organized as follows: first, an investigation of the achievable loop performances without and with filters is realized. Observations on the loop behavior then allow to derive an optimal selection procedure for the filters, resulting in good loop performance improvements. Robustness issues, choice of dither frequency and shape, and extent of possible integrator gain variations are also discussed. All results are validated in simulation on an ideal case study, with constant dynamics and an exact parabolic nonlinearity. Although the results presented here will be limited to this ideal case, they can be transposed as a tuning method for practical situations (time-varying dynamics and non-quadratic nonlinearities) as long as the uncertainties on the available model of the system remain within certain tolerance levels (discussed later in this paper). The ideas presented here were effectively applied by our group to such a situation (in [7]), being to our knowledge the first implementation of ESC on a real bioprocess.

For simplicity, only the scalar case (SISO) is considered. The static nonlinearity (output y, input θ) is expressed as:

$$y = h(\theta). \tag{1}$$

Fig. 1 shows the ESC loop configuration considered and all consistent notations for variables and transfer functions of associated components. $W_H(s)$ is a high-pass filter, and $W_L(s)$ is a low-pass filter. The cutoff frequencies of these filters are defined as ω_h and ω_l respectively. The dither signal $d(t)$ and demodulation signal $d_m(t)$ are periodic functions of period T (same shape, with possible phase differential) satisfying [2]:

$$\int_0^T d(t)\,dt = 0;\ P_d = \frac{1}{T}\int_0^T d^2(t)\,dt > 0;\ \max_{t\in[0,\,T]} |d(t)| = a \tag{2}$$

The dither is generally chosen as sinusoidal in shape, but other forms have also been investigated [2]. Its amplitude is noted a and its fundamental frequency is noted ω. Parameter δ is the ESC integrator gain at frequency ω. The high-pass filter output is termed $m(t)$ for later reference.

The dither amplitude will be kept constant throughout the paper to set a base of comparison. The nonlinear equilibrium input to output relation is the following exact parabolic map with a maximum at $(\theta^*, y^*) = (3, 9)$:

*Research supported by the Fonds Jinette-Côté (Telus company).

J-S. Deschênes is a professor of control engineering at the Université du Québec à Rimouski, Rimouski, QC, Canada (+1-418-723-1986 Ext. 1997; fax: +1-418-724-1879; e-mail: jean-sebastien_deschenes@uqar.ca).

P. N. St-Onge was an engineering Masters student under the supervision of professor J-S. Deschênes, and now holds a position as systems engineer at Ennesys in Nanterre, France (e-mail: pstonge@ennesys.com).

$$h(\theta) = 6\theta - \theta^2 \quad (3)$$

The following loop performance indicators are used:

- *Speed of convergence* is related to the time required by the loop to settle around the optimum (t_s).
- *Accuracy* is a measure of the variation on the output in steady-state around the optimum (ν):

$$\left| y(t) - y^* \right| \leq \nu \quad (4)$$

Finally, the notation $x(\omega t)$ is used to denote the contents of a given signal $x(t)$ at frequency ω (in the time domain).

Figure 1. Extremum seeking control scheme under consideration

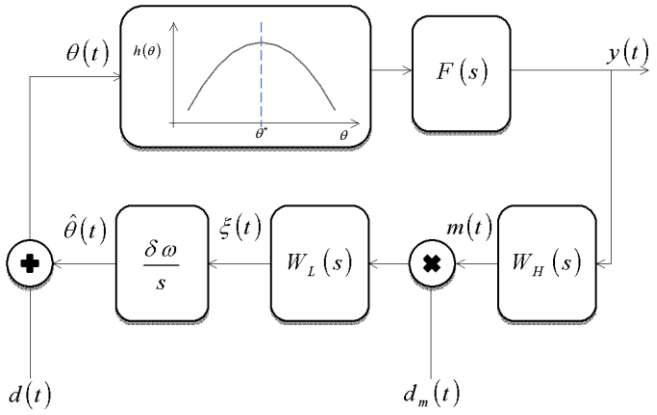

II. Extremum Seeking Fundamentals

In open-loop, under the static map assumption ($F(s) = 1$), sinusoidal variations on θ(t) impact the output $y(t)$ differently depending on its "situation" relative to the optimum (Fig. 2). The output generally appears as a sinusoidal signal similar to the input (in phase or 180° phase differential), except when it is operated exactly at the optimum, where frequency contents ω are no longer apparent on this signal. It is that basic static property that is exploited by the ESC algorithm. The gradient information stored in $y(\omega t)$ is then translated into a DC signal after demodulation for the integrator to act upon.

Figure 2. Open-loop sinusoidal responses of a static nonlinear mapping on various locations relative to the optimum

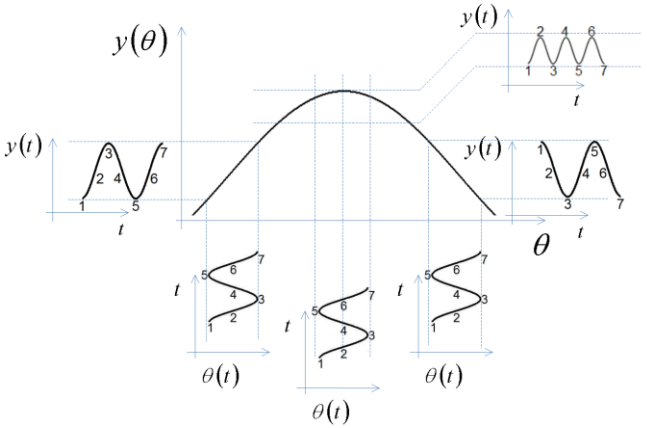

A. Performances for a static map without filters

Let $F(s) = 1$, ω = 0.1 rad/s, a = 0.4 (sinusoidal dither and $d_m(t) = d(t)$) and different values of δ for the analysis. Results are given in Table I, where it is seen that for all cases, the convergence rate is very slow (for this choice of ω, the static map assumption would hold even for $F(s) = 1/(1+s)$, which provides a better perspective). Higher values of δ do increase the convergence speed, but quickly degrade the accuracy.

TABLE I. Accuracy and Convergence Speed Results under the Static Map Assumption and without Filters

Parameter	Corresponding values at steady-state					
δ	0.02	0.05	0.1	0.2	0.4	1
ν	0.16	0.19	0.29	0.65	1.9	6.3
t_s (s)	~12 k	~5 k	~3 k	~1.5 k	~800	~200

B. Observations in the static map situation with filters

Introducing a high-pass filter in this case does not really improve convergence speed, but allows the accuracy to reach 0.16 in steady-state in all situations. This result is explained by complete DC rejection from the high-pass filter in steady-state, preventing additional contents of frequency ω to be fed back to the loop, which otherwise affect its overall behavior. When this is avoided, the dither signal affects the output as in the open-loop situation. Introducing a high-pass filter also allows to select higher values of δ. Simulations show that in many instances, values of δ > 1 are allowable. In such sense, the presence of the high-pass filter allows to further improve the convergence speed.

C. Demodulation Considerations

Demodulation translates the gradient information in $y(\omega t)$ (or more precisely, $m(\omega t)$) into a DC signal, which drives the algorithm towards the sought optimum. This is done through a multiplication between $d_m(t)$ and $m(t)$, where the matching frequency components produce a DC signal. For a sinusoidal dither ($d_m(t) = d(t)$) and $m(\omega t)$ having an amplitude b (which includes its sign) and phase ϕ (relative to $d(t)$), demodulation results in:

$$a\sin(\omega t)\times b\sin(\omega t-\phi) = \frac{ab}{2}\cos(\phi) - \frac{ab}{2}\cos(2\omega t-\phi) \quad (5)$$

This reveals the sensitivity of the ESC algorithm to phase ϕ. While demodulation is performed directly with the dither signal, the ideal case where ϕ = 0 is thus expected. When this is not the case, the performances may be affected, or perhaps even misled to "false" optimums: a 90° phase, for example, would result in a zero DC signal, making the ESC perceiving the system as operating at the optimum. Phases beyond ±90° would make the ESC deviate further away from the optimum as the DC signal would of the wrong sign. The importance of synchronizing the demodulation operation in non-ideal cases thus cannot be overemphasized.

As mentioned earlier, the demodulation step may impact the spectral contents being fed back to the loop. In classical

averaging analyses, exponentially decaying terms (due to the transfer functions involved) are always neglected. However, their impact during transients (thus on the ESC performance) is not always negligible, as their effect is also multiplicative [9]. An open-loop averaging analysis on this case (sinusoidal $d(t)$ of frequency ω) would reveal spectral contents at ω and 2ω, plus exponentially decaying terms in $m(t)$ (tied to $W_H(s)$ and $F(s)$ natural dynamics). Viewing the exponential term as a "temporary" DC term, demodulation generates contents of DC, ω, 2ω and 3ω frequencies. Frequency ω contents require special attention, as they may significantly impair the ESC performances. They arise from the presence of DC (thus the exponentially decaying term) and 2ω contents in $m(t)$. The latter is $O(a^3)$ and has negligible impact if a is *small*. The first term will be further investigated in the next section.

D. Impacts of exponentially decaying terms

From the previous open-loop averaging observations, let us consider an operation point $\bar{y}$ on $y(t)$, before any action (rejection) on this term by the high-pass filter. The frequency ω contents temporarily fed back to the loop are then:

$$\theta(\omega t) \;=\; d(\omega t)+\hat{\theta}(\omega t) \;=\; a\sin(\omega t)+a\,\delta\,\bar{y}\sin\left(\omega t-\frac{\pi}{2}\right) \quad (6)$$

where amplitude factor δ and phase $-\pi/2$ in the second term are due to the integrator. If this term is of significant amplitude, it may severely impact the loop performances, as the final characteristics of $\theta(\omega t)$ in closed-loop might become quite difficult to predict. If the second term is negligible, the only $\theta(\omega t)$ contents (even in closed-loop) originate from the dither signal: the averaging analysis for $y(\omega t)$ and $m(\omega t)$ can thus be based only on open-loop considerations.

The main avenues for rejecting the second term in (6) are (*i*) using small values of δ, (*ii*) applying a low-pass filter on $\xi(\omega t)$, and (*iii*) using a high-pass filter that quickly rejects $\bar{y}$. Small values of δ imply slow convergence dynamics, so does the low-pass filter option if it is to effectively get rid of the frequency ω contents. This leaves the high-pass filter option: however, a compromise should also be reached there, as too fast DC rejection dynamics would also reduce the amplitude of $y(\omega t)$, slowing the ESC convergence.

Recall the case from section II.A, with $\omega = 0.1$ rad/s and $a = 0.4$ under the static map assumption. Let $\delta = 0.4$, hardly an admissible value when no filter are used (Table I). For a low-pass filter to have a notable effect, its cutoff frequency ω_l should be selected (from (6)) so that:

$$a\,\delta\,\bar{y}\times\left|W_L(\omega)\right| \;<<\; a \quad (7)$$

A trial-and-error approach was used to determine the best closed-loop behavior for each case (individual use of high-pass or low-pass filter). Values of ω_h and ω_l near 0.01 rad/s were obtained. Results are shown in Fig. 3, where the high-pass filter alone shows better results than the low-pass filter alone. Their combined use is also shown in the figure. If the value of ω_h is modified from this setting, the performances decrease. If the value of ω_l is modified from this setting, the performances improve following its increase with best results as it nears infinity (or a time-constant of zero, equivalently as without the low-pass filter).

This result is of high importance, and indicates that if an optimal high-pass filter is found, the use of a low-pass filter is not only unnecessary, but is not recommended in regards to loop performances. This same conclusion about the use of low-pass filters is also reached for high-pass filters providing faster DC rejection. In such situations, as mentioned earlier, the averaging analysis for determining $y(\omega t)$ and $m(\omega t)$ can be based on open-loop considerations. The next section will discuss a selection procedure for the high-pass filter.

Figure 3. High-pass and low-pass filters under the static map assumption

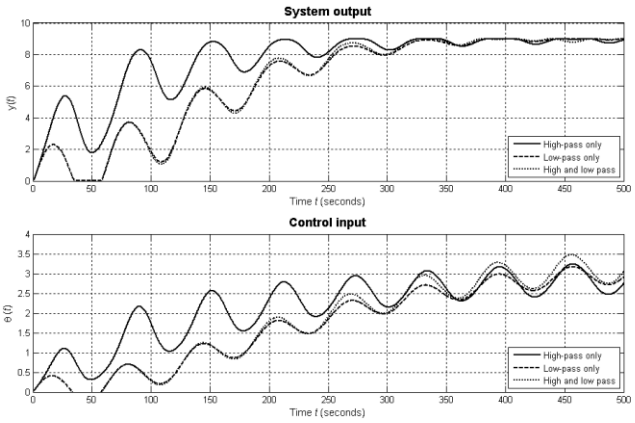

III. HIGH-PASS FILTER SELECTION

Previous results suggest that for fixed conditions on $F(s)$, ω, a and δ, there exists an optimal value of ω_h with regards to ES convergence dynamics, that prevents degradation of its accuracy and provides sufficiently "fast DC rejection" so its design can be based mainly on open-loop considerations. In particular, we are interested in developing such a selection methodology for non-negligible dynamics $F(s)$, as the case of the static map has already been solved (see [8]).

A. An optimal procedure for selecting ω_h

Under the previous observations, optimizing convergence rate can be done by a proper selection of the high-pass filter, exploiting its phase compensation possibilities while trying to minimize its attenuation impacts on $y(\omega t)$. In other words, this could be done by maximizing the amplitude of the DC signal after demodulation. Under this condition (for a fixed value of the integrator gain), the integrator action would be faster. Open-loop influences of $F(s)$ and $W_H(s)$ can be easily related to the parameters b and ϕ of $m(\omega t)$. For an example $F(s) = 1/(1+\tau s)$ and $W_H(s) = s/(\omega_h+s)$, the following relations are recovered:

$$\begin{aligned} b \;&\propto\; \frac{1}{\sqrt{1+\tau^2\omega^2}}\times\frac{\omega}{\sqrt{\omega^2+\omega_h^2}} \\ \phi \;&=\; \frac{\pi}{2} \;-\; \arctan\left(\frac{\omega}{\omega_h}\right) \;-\; \arctan(\tau\omega) \end{aligned} \quad (8)$$

The following expression for the DC signal is obtained:

$$\frac{ab}{2}\cos(\phi) \;\propto\; \frac{1}{\sqrt{1+\tau^2\omega^2}}\times\frac{\omega}{\sqrt{\omega^2+\omega_h^2}}\times\cos\left(\frac{\pi}{2}-\arctan\left(\frac{\omega}{\omega_h}\right)-\arctan(\tau\omega)\right) \quad (9)$$

This expression is to be maximized over ω_h for a given value of ω. While one could think about optimizing this expression for ω_h and ω simultaneously, this would not lead to an interesting result since the optimum of this surface is at $(\omega, \omega_h) = (0, 0)$. Thus, for a fixed value of ω, this leaves the following part of the expression to optimize over ω_h:

$$J(\omega_h) \;=\; \frac{1}{\sqrt{\omega^2+\omega_h^2}}\times\cos\left(\frac{\pi}{2}-\arctan\left(\frac{\omega}{\omega_h}\right)-\arctan(\tau\omega)\right) \quad (10)$$

This simple case leads to an analytical solution:

$$\omega_h \;=\; \omega\tan\left(\frac{1}{2}\arctan(\tau\omega)\right) \quad (11)$$

Comparative results for the output only (for an example situation where $\tau = 1$ s, $\omega = 1$ rad/s and $\delta = 0.4$) are shown in Fig. 4 for a few values of ω_h near the optimum. Convergence is fastest at the optimized value of ω_h (0.414 rad/s).

Figure 4. Convergence results for different choices of ω_h (first-order filter)

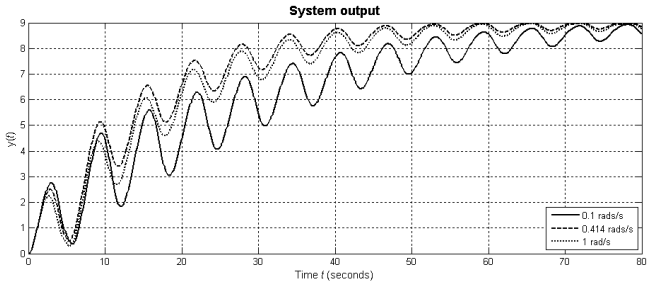

B. Higher-order filters and general case

In the literature about ESC, the high-pass filters used are limited to first-orders. To our knowledge, this is thus the first time the use of higher-order filters is considered. To limit the extent of our study, however, it is assumed that filters of the Butterworth type are best suited for the application, due to their "maximally flat" nature (minimal phase and amplitude fluctuations in the pass band). Such filters have the following transfer function structure:

$$W_H(s) \;=\; \frac{s^n}{D_n(s)} \quad (12)$$

where $D_n(s)$ is the n^{th} order Butterworth denominator polynomial function, parameterized by a cutoff frequency ω_h. Adapting the approach from section 3.1 to the general case for $F(s)$, the objective function (10) becomes:

$$J(\omega_h) \;=\; \frac{1}{\left|D_n(\omega)\right|}\cos\left(n\frac{\pi}{2}-\angle D_n(\omega)+\angle F(\omega)\right) \quad (13)$$

where $|\cdot(\omega)|$ and $\angle\cdot(\omega)$ refer to the norm and phase of the Laplace expression at frequency ω. Many results could be derived in a detailed case-by-case analysis of this expression. However, to keep our analysis short, we shall only consider the general first-order case $F(s) = 1/(1+\tau s)$ where a choice of $\omega = 1/\tau$ is made (an *a priori* estimated limit for fastest convergence). To assess the potential of higher-order filters in ES loops, we evaluate the result of applying criterion (12) to four filter orders. As Fig. 5 shows, selection of a second-order filter in this case has an advantage over a first-order (~15% increase on the DC amplitude of $\xi(t)$), while there remains little to gain from higher-order filters.

Figure 5. Objective function maximization versus filter order for first-order process dynamics $F(s)$ and choice of $\omega = 1/\tau$

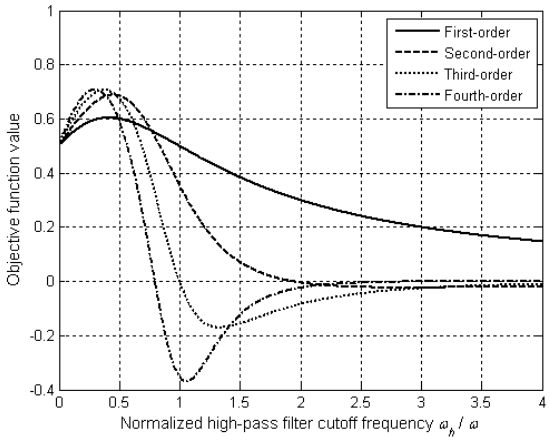

Further analysis of the results for this case provides more insight into the situation. Let $\tau = 1$, where the optimization procedure leads to $\omega_h = 0.414$ rad/s for a first-order filter and 0.452 rad/s for a second-order filter. The amplitude and phase effects of these filters are 0.92 and +22.5° (1st order), and 0.98 and +39° (2nd order). While the "ideal" filter would have an amplitude factor of 1.00 and a phase of +45°, the differences with the second order solution are essentially negligible. Fig. 6 shows comparative performances between these two situations, where results are indeed better with the second order filter.

Figure 6. ES dynamics with optimal first and second order filters ($\delta = 0.4$)

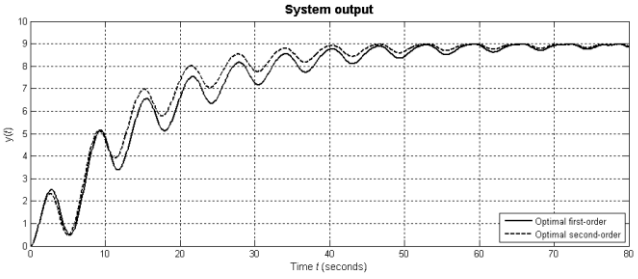

IV. Choice of the Dither Frequency

Knowledge about an optimal choice for ω_h allows better comparisons between different choices of ω and assessment of the impacts on the loop properties. Let the simple general

first-order system $F(s) = 1/(1+\tau s)$ be considered. Let $a = 0.4$, $\delta = 0.2$ and various sinusoidal dithers: $\omega = 0.2/\tau$, $0.5/\tau$, $1/\tau$, and $5/\tau$. Results are given in Fig. 7, where it can be seen that for fixed δ, the convergence speed generally increases with increasing values of ω, though rather limited gains seem to be obtained beyond $\omega = 1/\tau$. This is due to more important attenuation by $F(s)$ for higher values of ω, which eventually compensates for any gain to be obtained on that part.

Increased frequencies ω however allow higher values of δ to be selected. Fig. 8 shows the best results obtained with values of ω up to $10/\tau$. Achievable performances under this basic scheme of ESC seem to be limited by the step response of $F(s)$, similarly as in the case of the fast extremum-seeking scheme [14].

Figure 7. Results for different choices of ω with optimal second order high-pass filter for general first-order $F(s)$

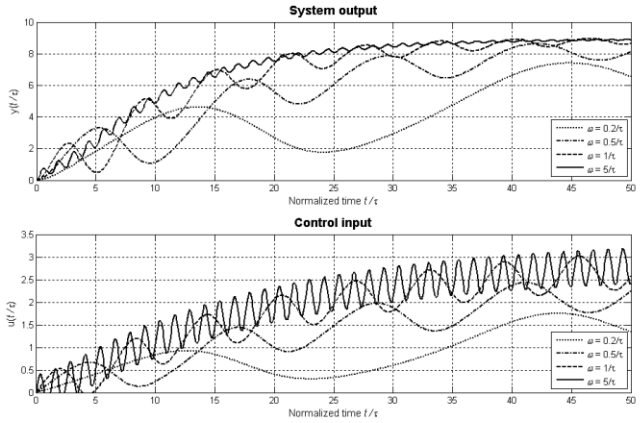

Figure 8. Achievable performances versus ω for general first-order $F(s)$

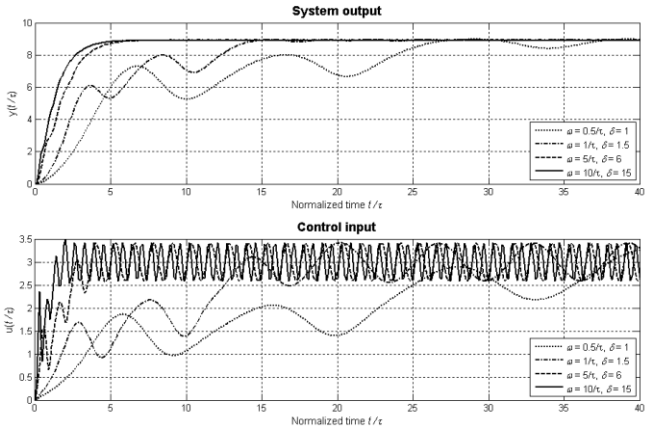

Phase sensitivity issues from section II.B however warns us that higher values of ω may imply even more sensibility to process parameter variations, as phase and frequency relate closely. This could also be the case about the nonlinearity characteristics of $h(\theta)$. However, the analysis in this paper will remain limited to the variations in $F(s)$.

A. Robustness analysis

This analysis considers the loop robustness as in relation to phase ϕ considerations from (5), to keep the real optimum as the attractor. Section II.B predicts that this will be the case as long as phase ϕ remains within $\pm 90°$. Let $F(s)$ be a general first-order system $1/(1+\tau s)$ nominally, in which an additional dead-time θ_d or time constant τ_2 may also be present (due to possible modeling errors):

$$F(s) = \frac{e^{-\theta_d s}}{(1+\tau s)(1+\tau_2 s)} \tag{14}$$

Different choices of $\omega\tau$ are considered. The variable $\Delta\phi$ is defined as a "phase margin" on ϕ towards $-90°$, in face of possible variations in $F(s)$. Since an exact first-order system cannot theoretically cause ϕ to reach $-90°$, this is why τ_2 and θ_d are introduced. Table II summarizes the situation and the maximum allowable values for τ_2 and θ_d (either occurrence only) before losing the ESC functionality.

TABLE II. ROBUSTNESS ASSESSMENT VERSUS DITHER FREQUENCY AND HIGH-PASS FILTER ORDER

$\omega\tau$	HF order	$\omega_h\tau$	$\Delta\phi$ (°)	$+\tau_2/\tau$	$+\theta_d/\tau$
5	1st	4.10	50.6	0.24	0.18
	2nd	3.43	72.7	0.62	0.25
1	1st	0.414	67.5	2.4	1.18
	2nd	0.452	83.8	9.5	1.46
0.5	1st	0.118	76.7	8.5	2.68
	2nd	0.148	88.0	57.3	3.07

Results show that robustness does indeed decrease as ω is increased. However a choice of $\omega = 1/\tau$ could very well be viable for a given first-order system, providing uncertainties remain in the range presented in Table II. A second order high-pass filter proves to be of interest, since in addition to providing faster response times, it also increases the ES loop robustness towards the uncertainties in $F(s)$.

These results also suggest the following design method for situations in which $F(s)$ is not exactly known: combining knowledge from the process operation and/or modeling from phenomenological equations, an expected average transfer function should be obtained. Then, a conservative estimate of expectable variations from this average situation should be determined. This uncertainty should then be translated into robustness requirements for the algorithm, which relates to the frequency selection (Table II). Once ω is chosen, ω_h is to be determined based on ω and the approximately known $F(s)$. In [17], complementary guidelines for tuning the ESC are provided for systems with dead time.

V. CASE OF A SQUARE WAVE DITHER

As reported in [8], the square wave dither is the most efficient dither signal form for fast convergence under the static map assumption, since its normalized power (P_d) is the maximum possible compared to any other form of excitation. A normalized square wave ($a = 1$) of fundamental frequency ω is expressed as follows:

$$\mathrm{sq}(\omega t) = \begin{cases} 1, & t \in \left[\dfrac{2\pi n}{\omega}, \dfrac{\pi}{\omega}(2n+1)\right] \\ -1, & t \in \left[\dfrac{\pi}{\omega}(2n+1), \dfrac{2\pi}{\omega}(n+1)\right] \end{cases} \quad (15)$$

where n is an integer. A Fourier series analysis reveals its frequency contents, at every odd multiple of ω:

$$\mathrm{sq}(\omega t) = \sum_{\substack{k=1 \\ (odd)}}^{\infty} \frac{4}{k\pi} \sin(k\omega t) \quad (16)$$

Each frequency component is affected in both amplitude and phase by $F(s)$ and $W_H(s)$. Noting b_k and ϕ_k respectively as the amplitude and phase of $m(k\omega t)$ and a_k as the amplitude of $d(k\omega t)$, the following expression for the DC part of the demodulated signal is found (for *small* values of a_k):

$$DC \propto \sum_{\substack{k=1 \\ (odd)}}^{\infty} \frac{a_k b_k}{2} \cos(\phi_k) \quad (17)$$

Since $a_k = a_1/k$, we obtain the following:

$$J(\omega_h) = \sum_{\substack{k=1 \\ (odd)}}^{\infty} \frac{|F(k\omega)|}{k^2} \frac{(k\omega)^n}{|D_n(k\omega)|} \cos\left(n\frac{\pi}{2} - \angle D_n(k\omega) + \angle F(k\omega)\right) \quad (18)$$

Applying this calculation up to the 19th harmonic of ω for $F(s) = 1/(1+s)$ results in $\omega_h = 0.426$ rad/s (1st order filter) and 0.459 rad/s (2nd order). Compared to those obtained for a sinusoidal dither (0.414 and 0.452 rad/s) it is expected the closed-loop behavior will not significantly improve by this "full spectrum consideration" design procedure. Thus, only its fundamental frequency ω can be considered for the filter selection. This is confirmed in Fig. 9, where a comparison is also provided between the sinusoidal and square wave dither signal results (ω = 1 rad/s, $a = 0.4$ and δ = 0.5).

Figure 9. Optimal second-order high-pass filters for sine and square wave dithers (fixed value of δ)

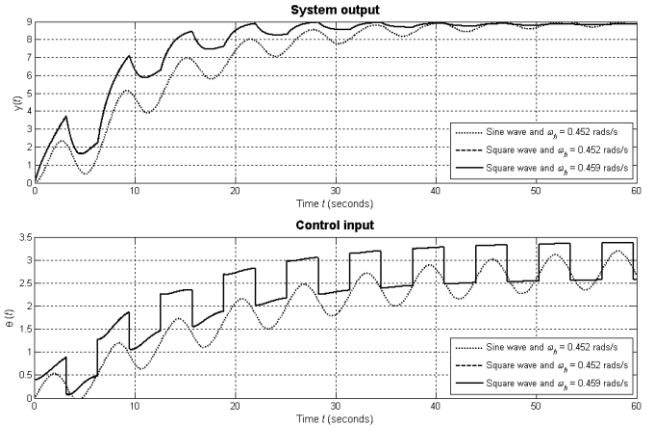

Pushing the performances to the limit as in Fig. 8 allows to make an interesting observation: despite the higher energy in a square wave, no additional gain is obtained by using this form over a sinusoid at this stage. The same maximum value of δ (for best performances) is allowable in both cases. From this point, further increasing δ decreases performances, until the loop becomes unstable. Results are shown in Fig. 10.

Figure 10. Optimal second-order high-pass filters for sine and square wave dithers (fixed value of δ)

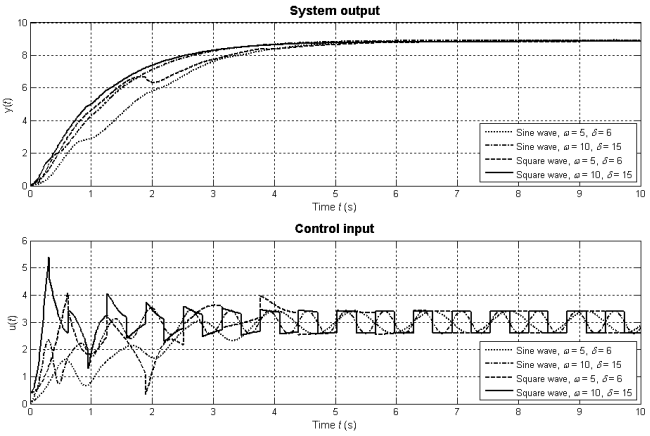

Other simulation results (not shown) prove the robustness issues towards uncertainties in $F(s)$ to be similar between the two cases (sinusoidal and square wave dithers).

VI. Comparisons with other loop improvements

This section will briefly address a comparison between this basic "optimized" version of ESC, and two recent loop improvement methods presented in [14] (fast ESC) and [15] (windowed integral method for derivative estimation). The following aspects will be investigated: brute performance assessment under knowledge of the exact model, robustness aspects under model uncertainty and noise sensitivity.

A. Performance comparisons

Let $F(s) = 1/(1+s)$, and a sinusoidal dither with $a = 0.4$. Two distinct scenarios where ω = 1 rad/s and ω = 5 rad/s are considered. For the basic ESC, optimal second-order high-pass filters are used ($\omega_h = 0.4523$ rad/s for ω = 1 rad/s, and $\omega_h = 3.432$ rad/s for ω = 5 rad/s). Tunings for the windowed method (using notation from [15]) are an integrator gain $K = a^2\omega\delta$, where δ = 1 for ω = 1 rad/s and δ = 1.5 for ω = 5 rad/s. For fast ESC, two tunings are considered for the Luenberger observer: the first has fast dynamics (triple pole at $s = -10$) with $L = [1000\ -970\ 299]^T$, and the second is as in [14] with $L = [0.237\ 0.343\ 0.167]^T$. Using the notation from [14], gain k was set at 0.4 for ω = 1 rad/s and $k = 1.2$ for ω = 5 rad/s. In both methods from [14] and [15], using notation from these papers, parameter ϕ was set to compensate exactly for the phase impact of $F(s)$, being $-\pi/4$ for ω = 1 rad/s and –atan(5) for ω = 5 rad/s.

Fig. 11 shows comparative performances for ω = 1 rad/s, while Fig. 12 shows the results for ω = 5 rad/s. The output y only is shown to reduce space requirements. Fig. 11 shows better performances for the fast ESC algorithm with the fast observation dynamics, while the other fast ESC (with slower observation dynamics) is a bit slower than the basic ESC. Slowest convergence is obtained with the method from [15]. When ω = 5 rad/s, convergence is still the fastest with the fast ESC with fast observer dynamics, followed by the basic ESC, method from [15] and finally fast ESC with the slower observer dynamics.

Figure 11. Optimal performance comparisons for ω = 1 rad/s

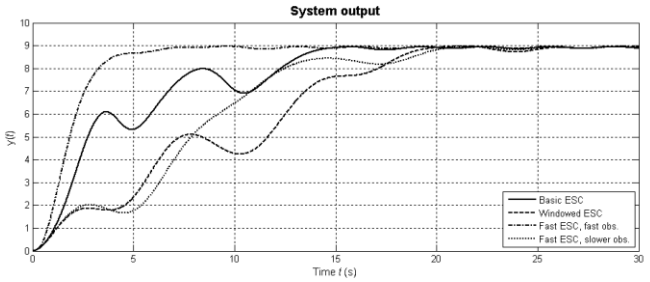

Figure 12. Optimal performance comparisons for ω = 5 rad/s

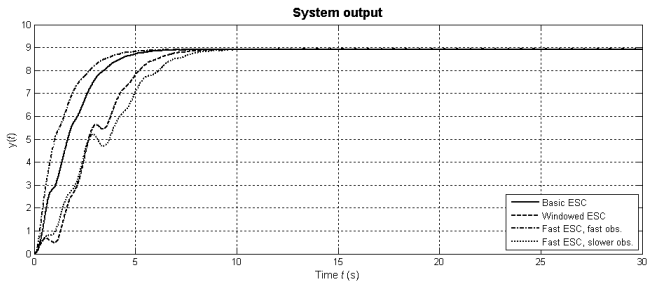

B. Robustness and noise sensitivity comparisons

Model uncertainty is considered in the form of a possible additional dead-time θ_d in $F(s)$ as in (14). Comparing results for ω = 1 rad/s show that fast ESC with fast observer gives the best results until $\theta_d = 0.3$ where all the algorithms have a similar behavior. The fast ESC with fast observation has a few difficulties for θ_d between 0.4 and 0.8, at which point all algorithms start again to behave similarly. At $\theta_d = 1.2$, only the basic ESC is slower (80 s) than the other three (40 s). At $\theta_d = 1.5$, only the fast ESC with slower observation and the windowed derivative estimator methods are stable. When $\theta_d = 1.6$ (and above), all algorithms are unstable.

For ω = 5 rad/s, the fast ESC with fast observation is best until $\theta_d = 0.1$. At $\theta_d = 0.15$, however, this algorithm becomes unstable. At 0.25, both this algorithm and the basic ESC are unstable, but the other two remain stable. All the algorithms are unstable for $\theta_d = 0.35$ (and beyond). The situation where $\theta_d = 0.2$ is shown in Fig. 13 for appreciation.

Figure 13. Performances under model uncertainty when $\theta_d = 0.2$

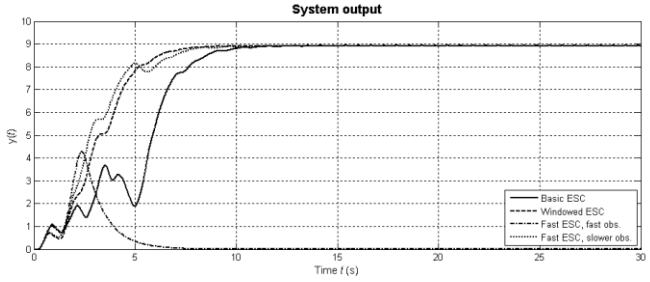

Noise sensitivity was also tested for all situations, for both input and output noise scenarios. While ω = 1 rad/s, all algorithms have a similar sensibility to either type of noise. While ω = 5 rad/s, the fast ESC (both observer tunings) has a significantly more important sensitivity to noise, in particular to auto-regressive (AR) noise. Fig. 14 shows the comparative results under knowledge of the exact model and with output AR noise while Fig. 15 shows the same for input noise. Low-pass filtered white noise is used for both situations (variance was set at 1 for the output noise and at 10 for the input noise, while the filter has a time constant of 0.1 s). The same noise signal was applied to each loop for fair comparison. Similar conclusions as in [15] are thus reached for higher ω.

Figure 14. Noise sensitivity of the ESC schemes under AR output noise

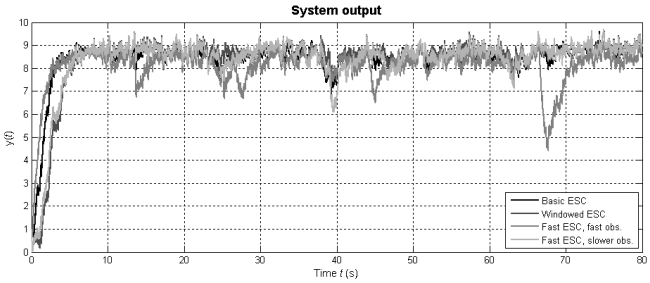

Figure 15. Noise sensitivity of the ESC schemes under AR input noise

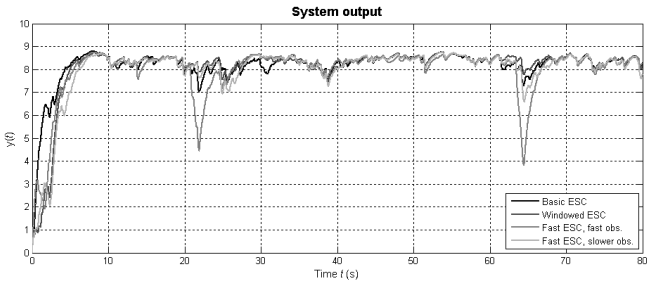

VII. CONCLUSIONS

This paper reviewed some of the foundations of the basic perturbation-based ESC scheme and developed a method for selecting its elementary components, significantly improving the loop performances. A comparative analysis with recently developed improvement methods showed that quite similar performances could be obtained using only the basic form of ESC (for strictly proper stable system dynamics) with similar robustness towards model uncertainty and noise sensitivity. As observed in these situations, the achievable performances for ESC on Wiener-Hammerstein systems remain limited by the step response of the system's natural dynamics. Square wave dither signals were also addressed; however, the results showed that for high dither frequencies and higher integrator gains, nothing is gained by using this dither signal form over a sinusoidal one. Finally, though the results were presented on an ideal well-characterized case (a necessary condition to obtain to determine the achievable performances), robustness aspects (model uncertainty) were addressed for applicability of the method to practical situations.

ACKNOWLEDGMENT

Authors would like to thank the Jinette Côté Foundation and the Telus company for supporting this research.

REFERENCES

[1] M. Krstić and H. H. Wang, "Stability of extremum seeking feedback for general nonlinear dynamic systems," *Automatica*, vol. 36, no. 4, pp. 595-601, Apr. 2000.

[2] Y. Tan, D. Nešić, I. Mareels, "On the choice of dither in extremum seeking systems: A case study," *Automatica*, vol. 44, no. 5, pp. 1446-1450, May 2008.

[3] D. Dochain, M. Perrier and M. Guay, "Extremum seeking control and its application to process and reaction systems: a survey," Math. Comput. Simul., vol. 82, no. 3, pp. 369-380, Nov. 2011.

[4] G. Gelbert, J. P. Moeck, C. O. Paschereit and R. King, "Advanced algorithms for gradient estimation in one- and two-parameter extremum seeking controllers," *J. Process Control*, vol. 22, no. 4, pp. 700-709, Apr. 2012.

[5] R. Becker, R. King, R. Petz and W. Nitsche, "Adaptive closed-loop separation control on a high-lift configuration using extremum seeking," AIAA J., vol. 45, no. 6, pp. 1382-1390, 2007.

[6] N. J. Killingsworth, S. M. Aceves, D. L. Flowers, F. J. Espinosa-Loza, and M. Krstić, "HCCI Engine Combustion-Timing Control: Optimizing Gains and Fuel Consumption Via Extremum Seeking," *IEEE Trans. Control Syst. Technol.*, vol. 17, no. 6, pp. 1350-1361, Nov. 2009.

[7] J. S. Deschênes, P. N. St-Onge, J. C. Collin and R. Tremblay, "Extremum Seeking Control of Batch Cultures of Microalgae *Nannochloropsis Oculata* in Pre-Industrial Scale Photobioreactors," in *Proc. 8th IFAC Int. Symp. Adv. Control Chem. Processes* (ADCHEM), Singapore, 2012, pp. 585-590.

[8] M. A. Rotea, "Analysis of multivariable extremum seeking algorithms," in *Proc. Am. Control Conf.*, Chicago, 2000, pp. 433-437.

[9] M. Krstić, "Performance improvement and limitations in extremum seeking control," *Syst. & Control Lett.*, vol. 39, no. 5, pp. 313-326, Apr. 2000.

[10] K. B. Ariyur and M. Krstić, "Multivariable extremum seeking feedback: analysis and design," in *Proc. Math. Theory Networks Syst.*, South Bend, 2002.

[11] H. H. Wang, M. Krstić and G. Bastin, "Optimizing bioreactors by extremum seeking," *Int. J. Adapt. Control Signal Process.*, vol. 13, no. 8, pp. 651-669, Dec. 1999.

[12] N. I. Marcos, M. Guay, D. Dochain and T. Zhang, "Adaptive extremum-seeking control of a continuous stirred tank bioreactor with Haldane's kinetics," *J. Process Control*, vol. 14, no. 3, pp. 317-328, Apr. 2004.

[13] L. Dewasme, A. Vande Wouwer, B. Srinivasan and M. Perrier, "Adaptive extremum-seeking control of fed-batch cultures of micro-organisms exhibiting overflow metabolism," in *Proc. 7th IFAC Int. Symp. Adv. Control Chem. Processes* (ADCHEM), Istanbul, 2009, pp. 165-170.

[14] W. H. Moase and C. Manzie, "Fast extremum-seeking for Wiener-Hammerstein plants," *Automatica*, vol. 48, no. 10, pp. 2433-2443, Oct. 2012.

[15] N. van de Wouw, M. Haring and D. Nešić, "Extremum-seeking control for periodic steady-state response optimization," in *Proc. 51st IEEE Conf. Decis. Control*, Maui, 2012, pp. 1603-1608.

[16] M. Chioua, B. Srinivasan, M. Guay and M. Perrier, "Dependence of the error in the optimal solution of perturbation-based extremum seeking methods on the excitation frequency," *Can. J. Chem. Eng.*, vol. 85, no. 4, pp. 447-453, Aug. 2007.

[17] J. S. Deschênes, "Demodulation Considerations in Extremum Seeking Control Loops," in *Proc. Am. Control Conf.*, Montreal, 2012, pp. 3389-3395.